AD_____

Award Number: W81XWH-04-1-0867

TITLE: A Myc-Driven In Vivo Model of Human Prostate Cancer

PRINCIPAL INVESTIGATOR: Simon W. Hayward, Ph.D.

CONTRACTING ORGANIZATION: Vanderbilt University Medical Center
Nashville, TN 37232-2765

REPORT DATE: October 2005

TYPE OF REPORT: Annual

PREPARED FOR: U.S. Army Medical Research and Materiel Command
Fort Detrick, Maryland 21702-5012

REPORT DOCUMENTATION PAGE

Form Approved
OMB No. 0704-0188

1. REPORT DATE	2. REPORT TYPE	3. DATES COVERED
01-10-2005	Annual	15 Sepl 2004 – 14 Sepl 2005

4. TITLE AND SUBTITLE

A Myc-Driven In Vivo Model of Human Prostate Cancer

5a. CONTRACT NUMBER

5b. GRANT NUMBER
W81XWH-04-1-0867

5c. PROGRAM ELEMENT NUMBER

6. AUTHOR(S)

Simon W. Hayward, Ph.D.

5d. PROJECT NUMBER

5e. TASK NUMBER

5f. WORK UNIT NUMBER

7. PERFORMING ORGANIZATION NAME(S) AND ADDRESS(ES)

Vanderbilt University Medical Center
Nashville, TN 37232-2765

8. PERFORMING ORGANIZATION REPORT NUMBER

9. SPONSORING / MONITORING AGENCY NAME(S) AND ADDRESS(ES)
U.S. Army Medical Research and Materiel Command
Fort Detrick, Maryland 21702-5012

10. SPONSOR/MONITOR'S ACRONYM(S)

11. SPONSOR/MONITOR'S REPORT NUMBER(S)

12. DISTRIBUTION / AVAILABILITY STATEMENT
Approved for Public Release; Distribution Unlimited

13. SUPPLEMENTARY NOTES

14. ABSTRACT

The long-term goal of the work proposed here is to generate, characterize and interrogate human epithelial cell-based in vivo models of prostatic carcinogenesis. These models will allow an examination of processes involved in carcinogenesis, tumor growth and metastasis. Since the tumors are themselves of human origin they represent an in vivo testbed to examine both tumor biology and the application of therapeutic agents. In the first year of funding we have published a description of the C7-myc model on which much of this proposal is based. We have qualified the proposed orthotopic grafting method to determine the metastatic spread pattern expected with human cells and we have generated and tested the tet-regulated constructs which are needed for aim 2. tissue recombinants using these constructs are now in mice. We have designed and validated retroviral vectors to drive shRNA for the suppression of PTEN in aim 3. This approach results in malignant transformation in SV40T immortalized cells and is being tested in a new set of low c-Myc expressing cells.

15. SUBJECT TERMS
tissue recombination, prostate cancer, in vivo, metastasis c-Myc, oncogene, model

16. SECURITY CLASSIFICATION OF:			17. LIMITATION OF ABSTRACT	18. NUMBER OF PAGES	19a. NAME OF RESPONSIBLE PERSON
a. REPORT	b. ABSTRACT	c. THIS PAGE			USAMRMC
U	U	U	UU	24	19b. TELEPHONE NUMBER *(include area code)*

Table of Contents

Annual Report
PCRP Idea Development Award
W81XWH-04-1-0867
A cMyc-Driven in vivo Model of Human Prostate Cancer

Introduction

The **long-term goal** of the work proposed here is to generate, characterize and interrogate human epithelial cell-based in vivo models of prostatic carcinogenesis. These models will allow an examination of processes involved in carcinogenesis, tumor growth and metastasis. Since the tumors are themselves of human origin they represent an in vivo testbed to examine both tumor biology and the application of therapeutic agents.

The first two aims will generate data on cancer development, androgen dependence, gene expression and patterns of metastatic spread prostate samples overexpressing cMyc. The third specific aim will use this information to target specific genes and normalize their expression in the Myc tumor. If a positive phenotype results the gene product may be a potential therapeutic target.

We are using a model in which human prostatic epithelial cells (huPrE) are grown in a tissue recombinant with rat urogenital sinus mesenchyme (rUGM) and grafted back into the in vivo environment of an intact male athymic rat host. Manipulations of the huPrE allow us to examine the effects of retroviral transfection with cMyc within the huPrE. Our original C7-Myc model forms aggressive tumors, hence, as originally proposed we are making lower expressing clones that will allow us to follow the progressive events in cancer initiation and progression. It is not possible to recover such samples from human patients, as it would require continued repeat biopsies with no medical/pharmaceutical intervention. It is highly desirable to study prostate cancer formation/progression in human prostatic epithelial cells, in an in-vivo setting, in order to minimize cell culture artifacts and more fully understand prostate cancer in vivo.

Body

The initial work proposed was a characterization of the C7-myc model of prostate cancer. The highly aggressive nature of the tumors resulting from the introduction of C7-myc into primary cultures of human prostatic epithelium, has been described in our first paper on this subject (Williams et al., 2005) (appended). These data strongly indicated that the development of models which moderated this effect was desirable if we were to generate data with relevance to human disease, rather than to an esoteric model system. Such an approach was proposed in specific aim 2. The development of such models early in the life of the award has been pursued aggressively as our initial findings suggest that this provides a better basis to understand the questions raised in aim 1, in a disease-relevant context, than the use of C7-myc cells as originally proposed. To this end we have generated and applied a tetracycline-regulatable lentiviral-based system as shown in figure 1. As shown this allows tetracycline-regulated expression of cMyc in a human prostate cell line. We have successfully infected primary cultures of huPrE with pLenti/TO/Myc and generated tissue recombinant grafts that are at present in animals. These experiments are ongoing to produce enough grafts for the experimental time points outlined in the grant proposal. Once these recombinants have aged expression of cMyc will be initiated by manipulating tetracycline levels in drinking water and the disease progression will be followed.

In addition to the regulatable cMyc vector a series of color marked vectors using the same basic construct have been generated as shown in figure 2.

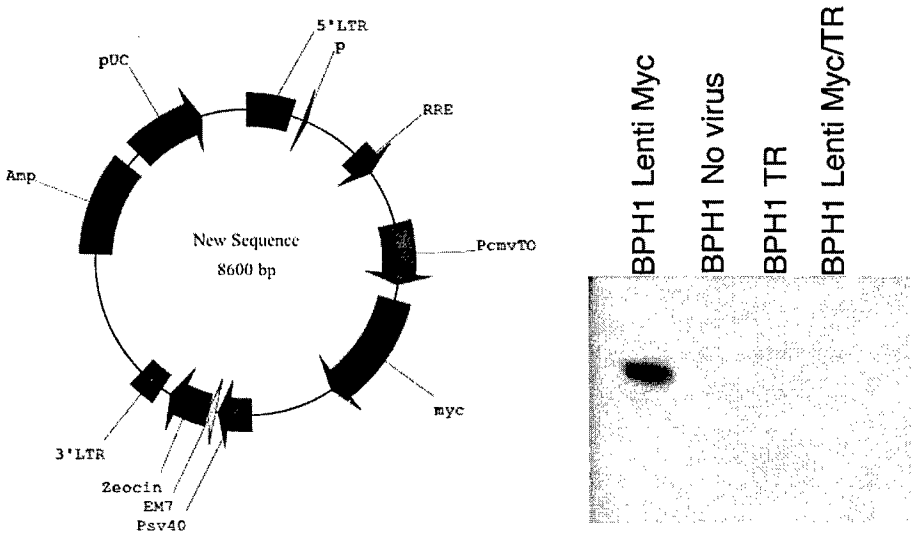

Figure 1. Tetracycline regulated lentiviral system for controlled expression of cMyc. *Left panel.* Plasmid map of pLenti/TO/Myc. This plasmid is constitutively active in absence of TR vector. *Right panel.* Western showing Myc expression from lentiviral infected human prostate epithelial cells. TR is the tet repressor which suppresses Myc expression in the absence of tetracycline

Three modified pLenti vectors have been created pLenti/TO/ V5 DEST EGFP. pLenti/TO/ V5 DEST ECFP, pLenti/TO/ V5 DEST DsRed2

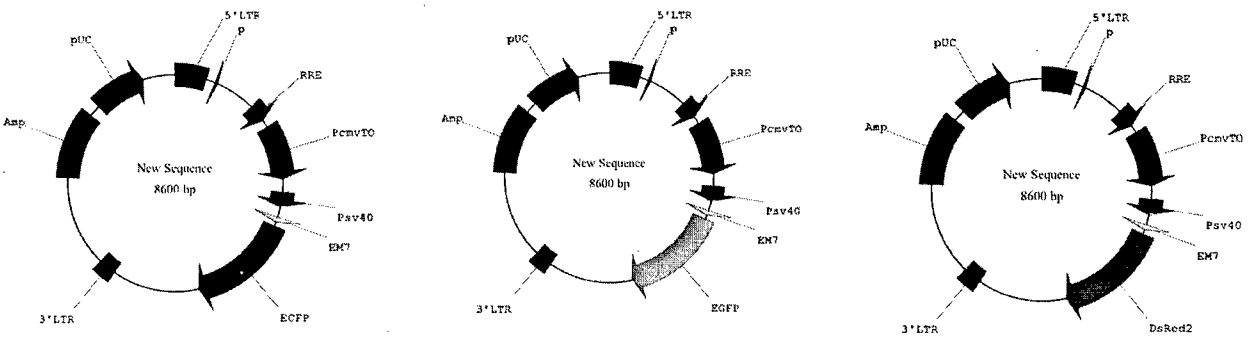

Figure 2. PLenti4/TO/v5-Dest clones carrying different color markers. This allows us to use multiple vectors in one graft. The different color markers allow us to track cells and EGFP and DsRed have specific antibodies raised against them (the closely related green and blue colors cannot be separated immunohistochemically). Color markers allow us to visualize infection efficiencies and are unaffected by the presence of TR vector or tetracycline.

In order to more efficiently track metastatic lesions, as proposed in specific aim 1 we have utilized a trifusion protein generated at Stanford University (Ray et al., 2004). This protein has been designed for cell and metastasis tracking and provides a number of technical advantages over the GFP-based method proposed in the original application. Thus this development does not change the aims but should increase the ability to achieve them. The trifusion protein has been introduced into a lentiviral vector (figure 3) and has been successfully tested in vitro. In vivo testing is about to commence.

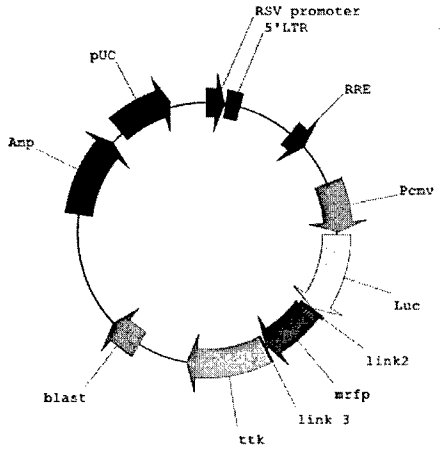

Figure 3. The Lenti Tri fusion was developed from the pcDNA trifusion vector (kind gift from Dr. Ray, Stanford) This vector was created to allow us to follow metastatic spread in the C7-Myc or other newly-developed cell lines. The Vector gives strong red fluorescence and is positive on luciferase assays. We have not yet tested our construct in mice but the original construct has been used by Dr. Ray's group to image lesions.

As an alternative promoter to drive cMyc expression we are testing the ARR_2PB promoter (Zhang et al., 2000) (figure 4). This promoter, developed by Dr. Robert Matusik at Vanderbilt, should allow for androgen-dependent expression of cMyc in tissue recombinants. This provides another alternative to the proposed cmv and tet-regulated systems. Should this prove unsuccessful the PSA promoter also exists as an alternative.

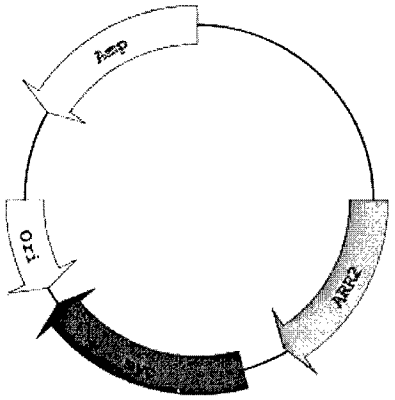

Figure 4. The ARR_2PB-Myc system is being developed. The ARR_2PB promoter is an androgen dependent prostate specific promoter that will drive high expression of Myc only in the luminal cells of the prostate grafts. This will be developed into either a lentivirus or retroviral construct.

In specific aim 3 we proposed to suppress the expression of PTEN. We have designed and validated retroviral vectors to drive shRNA for the suppression of PTEN. This approach results in malignant transformation in SV40T immortalized cells and is now undergoing initial testing in primary cultures of human prostatic epithelial cells.

A collaboration has been established with Dr. Chalfant, Virginia Commonwealth University, to use the C7-Myc virus in a grant proposal on Sphingolipid Regulation of Caspase 9 Alternative Splicing.

Technical Modifications:

The use of lentiviral as compared to retroviral approaches has been pursued. This reflects technological advances in viral methodologies and the use of a system in which infectivity is more efficient. The general approaches to be used are unchanged by this modification.

The use of a trifusion peptide rather than GFP as originally proposed allows increased sensitivity and more efficient tracking of metastatic lesions. Again this does not affect the overall aims of the proposal but rather the general trend of improvement in the tools available.

Personnel Changes

None

Key Research Accomplishments

One of the important proposed methods was to develop a tetracycline-inducible system to examine prostate cancer progression. This has been achieved. The tissue recombinant grafts of tetracycline inducible Myc are in animals, these will constitute the longest time point of possibly close to 1 year.

In a development from the proposed technology, reflecting technological improvements in the field, lentiviral (rather than retroviral) constructs have been constructed that allow transfer of Myc in a tetracycline responsive plasmid (figure 1). The original clone created had a 2bp insert immediately adjacent to the ATG start site that was not initially discovered on DNA sequencing. A new clone has now been extensively DNA sequenced and expression of Myc verified by RT-PCR and Western blot. (figure 1)

We have successfully Infected the prostatic BPH1 cell line with pLenti Myc and shown repression of Myc expression with introduction of TR vector. We have constructed several color expression clones for use in this and other projects. These expand our potential use of the commercially available vectors that at present contain only Zeo resistance.

We have created a lentiviral clone specifically for imaging of metastatic lesions. The luciferase can be imaged using light detectors. Ttk allows PET scanning and mRFP emits a wavelength of light that can penetrate deeper into the mouse tissues to give a signal from internal sites, especially the bone grafts our host mice carry.

We have characterized the use of orthotopic grafting as an improvement on the use of sub-renal capsule grafting to examine the metastatic process. These studies indicate that the orthotopic site has considerable advantages in such applications, and will therefore be used in some specific applications as required by experimental protocols.

Reportable Outcomes.

Papers

Williams, K., Fernandez, S., Stien, X., Ishii, K., Love, H.D., Lau, Y-F., Roberts, R.L., Hayward, S.W. (2005) Unopposed c-MYC expression in benign prostatic epithelium causes a cancer phenotype. Prostate 63, 369-384 (appended)

Presentations

Karin Williams, Kenichiro Ishii and Simon W. Hayward. (2004). Unopposed c-MYC expression in benign prostatic epithelium causes a cancer phenotype. SBUR 2004 Fall Meeting in Urologic Research Savanna ,GA USA Dec 9-Dec 12

Karin Williams, Kenichiro Ishii and Simon W. Hayward. (2004) c-Myc Overexpression In Human Prostate Initiates Cancer In Vivo. 10th Prouts Neck Prostate Cancer Meeting. Portland Maine Nov. 4-7

Karin Williams, Kenichiro Ishii and Simon W. Hayward. (2004) c-Myc Overexpression in Human Prostate epithelial cells Initiates Cancer in a tissue recombinant model. 3rd Joint Host-Tumor Interactions Program & Department of Cancer Biology Retreat, Lake Barkley, Kentucky. Nov 13-15

Cell lines

Human prostatic epithelial cells overexpressing cMyc under a cmv promoter (C7-myc) have been generated and are described in the published paper (Williams et al, 2005 - appended). These cells are available for distribution to non-profit institutions upon request. In the event of requests from for-profit organizations appropriate licensing agreements will be established.

Conclusions.

This work is proceeding slightly behind the predicted timeline. A number of changes to the specific details of the original statement of work are noted. These reflect technical methodological improvements that enhance the overall quality of the proposal. None of these changes alters the overall aims and long-term goal of the proposed work but have required that we delay some proposed experiments while developing new tools. The tool development stage is now effectively completed, subject to technological changes which may occur, and the in vivo biological studies have started.

References

Ray, P., De, A., Min, J. J., Tsien, R. Y., and Gambhir, S. S. (2004). Imaging tri-fusion multimodality reporter gene expression in living subjects. Cancer Res *64*, 1323-1330.

Williams, K., Fernandez, S., Stien, X., Ishii, K., Love, H. D., Lau, Y. F., Roberts, R. L., and Hayward, S. W. (2005). Unopposed c-MYC expression in benign prostatic epithelium causes a cancer phenotype. Prostate *63*, 369-384.

Zhang, J., Thomas, T. Z., Kasper, S., and Matusik, R. J. (2000). A small composite probasin promoter confers high levels of prostate- specific gene expression through regulation by androgens and glucocorticoids in vitro and in vivo. Endocrinology *141*, 4698-4710.

The Prostate 63:369–384 (2005)

Unopposed c-MYC Expression in Benign Prostatic Epithelium Causes a Cancer Phenotype

Karin Williams,[1]* Suzanne Fernandez,[1] Xavier Stien,[1] Kenichiro Ishii,[1] Harold D. Love,[1] Yun-Fai (Chris) Lau,[5] Richard L. Roberts,[1,2,4] and Simon W. Hayward[1,3,4]

[1]Department of Urologic Surgery, Vanderbilt University Medical Center, Nashville, Tennessee
[2]Department of Pathology, Vanderbilt University Medical Center, Nashville, Tennessee
[3]Department of Cancer Biology, Vanderbilt University Medical Center, Nashville, Tennessee
[4]Department of Vanderbilt-Ingram Comprehensive Cancer Center, Vanderbilt University Medical Center, Nashville, Tennessee
[5]Department of Medicine, VA Medical Center, University of California, San Francisco, California

BACKGROUND. We have sought to develop a new in vivo model of prostate carcinogenesis using human prostatic epithelial cell cultures. Human prostate cancers frequently display DNA amplification in the 8q24 amplicon, which leads to an increase in the copy number of the c-MYC gene, a finding that suggests a role for c-MYC in human prostate carcinogenesis. In addition overexpression of c-MYC in transgenic mouse models results in prostatic carcinogenesis.
METHODS. We took advantage of the ability of retroviruses to integrate foreign DNA into human prostatic epithelium (huPrE) to generate cell lines that overexpress the c-MYC protooncogene. These cells were recombined with inductive rat urogenital sinus mesenchyme and grafted beneath the renal capsule of immunocompromised rodent hosts.
RESULTS. The resultant tissue displayed a phenotype consistent with a poorly differentiated human prostatic adenocarcinoma. The tumors were rapidly growing with a high proliferative index. The neoplastic cells in the tumor expressed both androgen receptors (AR) and prostate-specific antigen (PSA), both characteristic markers of human prostate cancers. Microarray analysis of human prostatic epithelial cells overexpression c-MYC identified a large number of differentially expressed genes some of which have been suggested to characterize a subset of human cancers that have myc overexpression. Specific examples were confirmed by Western blot analysis and include upregulation of c-Myb and decreased expression of PTEN. Control grafts using either uninfected huPrE or using huPrE cells infected using an empty vector expressing a green fluorescent protein tag gave rise to well differentiated benign prostatic glandular ducts.
CONCLUSIONS. By using a retroviral infection strategy followed by tissue recombination we have created a model of human prostate cancer that demonstrates that the c-MYC gene is sufficient to induce carcinogenesis. *Prostate 63: 369–384, 2005.* © 2004 Wiley-Liss, Inc.

KEY WORDS: **myc; tissue recombination; retroviral gene transfer; prostate cancer**

Grant sponsor: University of California, San Francisco Prostate Cancer Center; Grant sponsor: DAMD; Grant number: 17-01-1-0037; Grant sponsor: NIH; Grant number: CA96403; Grant sponsor: Davis Foundation; Grant sponsor: Vanderbilt Ingram Cancer Center; Grant number: P30 CA68485; Grant sponsor: Vanderbilt Diabetes Research and Training Center; Grant number: P60 DK20593.

*Correspondence to: Karin Williams, Department of Urologic Surgery, A1302 MCN, Vanderbilt University Medical Center, Nashville, TN 37212-2765. E-mail: karin.williams@vanderbilt.edu
Received 25 May 2004; Accepted 7 September 2004
DOI 10.1002/pros.20200
Published online 21 December 2004 in Wiley InterScience (www.interscience.wiley.com).

INTRODUCTION

Prostate cancer is the single most diagnosed cancer in men and a major cause of mortality/morbidity within North America and Europe [1–3]. The introduction of routine PSA testing has resulted in earlier detection of prostate cancer and appears to be resulting in a decrease in disease-specific death rates [4]. While certain proteins such as TSPY have been found to display altered expression in very early cancer [5], there has not been sufficient characterization of PCa to identify many potential progression pathways that characterize prostate cancer [6]. Therefore, unlike the well-characterized pathway of acquired mutations displayed by colon cancer, there is not a clearly defined pathway for the progression and development of malignant disease in the prostate.

c-MYC is a transcription factor that belongs to the myc/mad/max family of Basic-helix-loop-helix-zipper (bHLHZ) proteins. Three closely related members make up the MYC family (c-MYC, L-MYC, N-MYC) and although they have very distinct patterns of expression, evidence exists that the proteins are able to compensate, to some extent, for the loss of one family member [7]. However, both c-MYC and N-myc knockout mice exhibit embryonic lethality [8,9].

Myc forms a heterodimeric transcription factor complex with its partner Max [10]. In this state Myc/Max is capable of binding to its DNA recognition site, the so-called E-box [core sequence (CACGTG)]. Max/Mad heterodimers also bind the E-box and act as transcriptional repressors presumably repressing genes induced by Myc/Max [11]. Like myc, both Max and Mad have related family members, capable of modulating this pattern of induction/repression by binding to each other and modulating the availability of the E-box. Myc also appears to be capable of binding and sequestering several other regulatory factors such as Sp-1 and Miz-1, causing transcriptional modulatory effects not associated with E-box binding [12–14].

Cell proliferation, differentiation, and apoptosis are all responses regulated by myc expression. The Myc protein acts as a cell activator that relies on other accessory proteins to specify the nature of the response. The proliferation pathway is mediated by Myc's ability to activate several cyclins, including cyclin E [15] and cyclin D2 [16,17]. The activation of cyclin D2 causes sequestering of $p27^{kip}$ from cyclin E and driving the cell into S phase. Myc also indirectly reduces expression of $p21^{WAF1}$ and $p15^{ink4b}$ [18,19], both of which are involved in cell cycle arrest.

Myc overexpression/deregulation has been implicated in numerous neoplastic transformations both in human disease and transgenic mouse models [20–28]. Furthermore, inactivation of the myc gene has been shown to elicit regression of Myc-induced tumors in the absence of novel mutations [23,29,30].

c-MYC was the first oncogene to be recognized as being overexpressed in human prostate cancer [28]. However, the precise role played by c-MYC in human prostate cancer is unclear in part due to the amplification of the 8q24 amplicon. This amplicon is particularly rich in genes, several of which [e.g., c-MYC [31], NOV [nephroblastoma overexpressed gene], EIF3S3 [eukaryotic translation initiation factor 3 subunit 3], HAS2 [hyaluronan synthase2] [32], KIAA0196 [33], and PSCA [34]] are expressed in prostate and have either oncogenic or tumor suppressor potential. FISH analysis has identified amplification of the 8q24 amplicon [32,35–37] in a large percentage of human adenocarcinomas [38,39] and some prostate intraepithelial neoplasias (PIN) [37].

Mouse models of prostatic neoplasia have been generated in which the c-MYC gene was expressed from either the probasin promoter [20] or C(3)1 promoter [22]. Two probasin promoter variants were used in one study; these promoters share the same prostate specificity but differ in promoter activity. Both the Hi-Myc (ARR_2PB-myc) and Low-Myc (sPB-myc) animals develop mouse PIN (mPIN) and invasive carcinoma but the time to development and progression differs by approximately 6 months [20]. While these probasin-Myc transgenic mice apparently progress from mPIN to prostatic adenocarcinoma the relationship of PIN to adenocarcinoma in humans remains unsubstantiated. The C(3)1 promoter is a weaker promoter than the probasin constructs. Mice carrying the C(3)1-Myc transgene fail to develop adenocarcinoma within their lifetime although they do develop mPIN-like lesions [22]. These data suggest that a low level of myc expression correlates with mPIN development while the progression to adenocarcinoma requires elevated c-MYC levels.

Given that c-MYC is reported to be overexpressed and the gene amplified in human prostate cancer, and because transgenic mouse models overexpressing c-MYC in the prostate have a dose related progression towards malignancy, we decided to test the ability of cMYC to transform human prostatic epithelium. To do so in vivo a tissue recombination model was used to follow prostatic carcinogenesis in response to overexpression of c-MYC.

MATERIALS AND METHODS

Human Cell Culture

Human prostate tissue samples were obtained from the Vanderbilt Tissue Acquisition Core via the Department of Pathology in accordance with Vanderbilt IRB protocols. Cores 6 mm in diameter were removed from

radical prostatectomy samples and were sampled by histologic analysis on frozen sections to determine the nature (benign vs. malignant vs. severe inflammation) of the tissue contained within the core.

Benign tissue was cut into 2 mm cubes using sterile scalpels. After washing in RPMI (Gibco, Carlsband, CA) 5% FCS (Atlanta Bioscience Atlanta, GA) the tissue was plated on Primaria™ tissue culture flasks with sufficient medium to wet the plate and create a strong surface tension (1.2 ml/25 cm^2). After cell attachment had taken place (~12 hr) the volume of medium was increased. Tissue obtained from tissue recombination grafts was reintroduced into culture in an identical manner.

Tissue Culture Medium

Tissue culture medium for human prostatic epithelial cells (huEpi mix) consisted of: [RPMI 1640, 1% ITS (Insulin Transferrin Selenium), 1% Antibiotic/Antimycotic (all from Gibco)], 2.5% charcoal stripped serum (Atlanta Bioscience), BPE (Bovine Pituitary Extract) 1:250 (Hammond Cell Tech, Winsor CA), Cholera toxin (1 μg/ml), and Epidermal Growth Factor (0.01 μg/ml) (Sigma, St. Louis, MO).

LZRS Retroviral Plasmid Construct

The plasmid LZRS c-MYC/EGFP (Fig. 1) was constructed utilizing the LZRS-EGFP backbone (Nolan Laboratory, Stanford, CA). The CMV promoter was excised from pIRES-EGFP (Clontech, Palo Alto, CA) as a BglII/BamHI fragment. The fragment was ligated into the BamHI site of the LZRS-EGFP backbone to give C7Δ.

The human c-MYC cDNA clone (BC000917) was obtained from ATCC (Rockville, MD) and amplified by PCR using a 5′ primer specific to translational start site and a 3′ primer containing an XhoI restriction site and the consensus sequence for the translational stop site with subsequent deletion of any polyadenylation sites. After PER amplification, the product was gel purified, and cloned into poem T-Easy (ProtÕgÕ, Madison, WI). Following DNA sequence verification of the cloned product the c-MYC coding region was excised using EcoRI/XhoI and sub cloned into the EcoRI/XhoI sites of pLZRS-EGFP to give C7-Myc.

Viral Production

Amphotrophic ϕNXA packaging cells were obtained from ATCC [under an MTA from the Nolan laboratory Stanford (www.stanford.edu/group/nolan)]. These cells were maintained in 5% FCS/RPMI 1,640 with antibiotic surveillance. The ϕNX packaging cell lines were reselected with both hygromycin B and diphtheria toxin (Sigma) every 3–4 months. The LZRS retroviral constructs were transfected into ϕNX cells that were 70%–80% confluent. Routine transfection took place using 25 cm^2 flasks. Lipofectamine 2000 (Invitrogen, Grand Island, NY) was optimally used at a

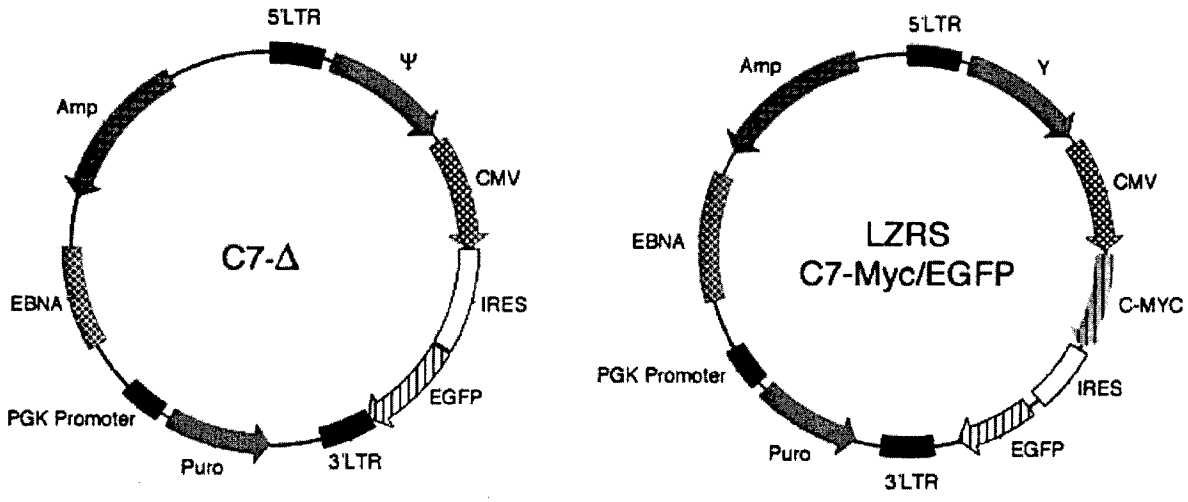

Fig. 1. Retroviral constructs, control vector C7Δ and LZRS C7-MYC/EGFP. pLZRS is a retroviral vector derived from the Moloney murine Leukemia virus (MoMuLV). The gene of interest (c-MYC) and the Enhanced Green Fluorescent Protein (EGFP) are expressed from a bicistronic message under the control of the cmv promoter. The 5′ viral LTR controls expression of the transcript that contains Ψ (the extended viral packaging signal). The retroviral particle contains, and integrates into the genome, only the genetic information between and including the 5′ and 3′ LTRs'. pLZRS does not contain the structural genes necessary for viral formation and replication, these are provided by the packaging cell line ϕNX. Other components of pLZRS such as the puromycin resistance gene and EBNA (EBV episomal functions) contribute to stability and selection of the plasmid in the packaging cell line. pLZRS also includes the pUC origin of replication and E. coli Amp gene for propagation and antibiotic selection in bacteria.

final concentration of 3 μl/ml according to manufacture's protocols. Eight hours post transfection the ϕNX cells were given fresh RPMI/5% FCS and incubated overnight at 37°C. Viral supernatant was removed in the morning and the cells split if necessary and moved to a 32°C incubator to ensure greater viral stability. The viral supernatant was spun at 3,000 rpm and passed through a 45 μm filter to ensure the absence of contaminating ϕNX cells. The viral supernatant was then supplemented with 4 μg/ml Polybrene (hexadimethrine bromide, Sigma) and either stored at −70°C or used immediately.

Viral Infection

The viral supernatant containing the c-MYC/EGFP or C7-delta control retrovirus was diluted 1:1 with huEpi mix that was double strength with respect to the added constituents and the polybrene concentration was corrected to 4 μg/ml. The viral medium was then placed on the huPrE cells (three patients from which both TZ and PZ cores were put into independent culture dishes in duplicate) in culture and replaced 8 hr later. Primary cells were incubated at 37°C as their rate of cell division was severely compromised at 32°C, the increased stability of the viral particles at 32°C therefore could not be utilized when working with huPrE but proved useful when certain immortal cell lines were infected, data not shown. Successive rounds of infection over 5 days were employed to generate infected cells. Owing to the growth patterns of the huPrE we found that daily infection would ensure the presence of virus during the initial outgrowth of cells and therefore generate the maximum number of infected cells. Infection rates were monitored using fluorescence microscopy of the bicistronic EGFP tag. After infection the cells were maintained in culture until use. The cells were examined by a clinical pathologist to assess any phenotypic differences in the infected cells.

Culture of Infected Cells

Following infection, a proportion of the cells were used as a source of epithelium in tissue recombinants. The remaining cells were maintained in culture for a further 16 passages with batches frozen in liquid nitrogen at different points. All remaining cells were frozen after passage 16. Cells were examined for the continued expression of the EGFP tag using fluorescence microscopy; expression of AR, PSA, and c-MYC was monitored using Western blot analysis.

Tissue Recombination

Tissue recombinants were prepared, as previously described [40,41]. Briefly, pregnant rats were obtained from Harlan (Harlan, Indianapolis). Rat urogenital sinus mesenchyme (UGM) was prepared from 18-days embryonic fetuses (plug date denoted as day 0). Urogenital sinuses were dissected from fetuses and separated into epithelial and mesenchymal components by tryptic digestion, as previously described. UGM was then further reduced to single cells by a 90 min digestion at 37°C with 187 U/ml collagenase (Gibco). Following digestion, the cells were washed extensively with RPMI-1640 tissue culture medium. Viable cells were then counted using a hemacytometer, with viability determined by trypan blue exclusion. Epithelial cells were released from tissue culture plates using trypsin. Trypsin was neutralized and the cells washed and counted using a hemacytometer. Cell recombinants were prepared by mixing 100,000 epithelial cells with 300,000 stromal cells. Cells were pelleted and resuspended in 50 μl of neutralized type 1 rat tail collagen prepared as, previously described [42]. The recombinants were allowed to gel at 37°C for 15 min and were then covered with growth medium and cultured overnight. They were then grafted beneath the renal capsule of adult male severe combined immunodeficient (SCID) mice [C.B.17/IcrHsd-scid mice (Harlan)].

Subcutaneous Grafting

Epithelial cells (100,000) were pelleted and resuspended in 50 μl of neutralized type 1 rat tail collagen prepared, as described previously [42] and placed under the skin of adult male SCID mice [C.B.17/IcrHsd-scid mice (Harlan)]. Some of these subcutaneus grafts were surrounded in matrigel (BD Biosciences, Bedford, MA) at the time of grafting.

Tissue Recovery, Fixation, and Processing

Mice were sacrificed by Isoflurane inhalation followed by cervical dislocation according to Vanderbilt animal care protocols. The kidney and attached graft together with internal organs were removed and examined at the gross level. The c-MYC grafts owing to their substantial size were divided into several pieces. Those fragments containing the kidney were fixed in 10% neutral buffered formalin, as were the internal organs of the host. The remaining tissue was then divided to give representative portions for (1) RNA extraction, (2) Protein extraction, and (3) for further tissue culture. Tissue destined for RNA extraction was cut into small pieces and immersed in RNA LATER (Ambion, Austin, TX) according to manufacturer's instructions. Tumor tissue for protein extraction was snap frozen on dry ice and stored at −70°C until required. The third portion of the tumor was removed

for tissue culture or frozen [43] to allow extraction of viable cells.

Culture of Tumor-Derived Epithelial Cells

Tumor tissue was minced and placed in culture in a minimal volume of tissue culture medium (as per primary culture). Cells were passaged using trypsin and then frozen. Continued transduced gene expression in these cells was confirmed by fluorescence microscopy to detect the expression of EGFP and by Western blotting to confirm continued expression of c-MYC.

Antibodies

For immunolocalization studies the following antisera were used. Androgen receptors (AR) were detected using a rabbit polyclonal antibody (*sc*-816) raised against a peptide within the N-terminal domain of hAR, EGFP was detected using a mouse monoclonal to the full length GFP that detects all GFP variants (*sc*-9996). c-Myb (*sc*-8412), PTEN (*sc*-7974*sc*-9996), p63 (*sc*-8343) (Santa Cruz Biotechnology, Santa Cruz, CA). c-MYC was detected using a mouse monoclonal (NCL-c-MYC) raised against full-length recombinant human protein obtained from Novocastra (Burlingam, CA). Ki67 (M-7240), PSA (A-0562), broad-spectrum Keratin antibodies (Z-0622) were obtained from DAKO (Carpinteria, CA), and keratin 8, 14, and 18 [clones LE41, LL001, and LE61 gifts from Prof. E.B.Lane, Dundee University, UK [44,45]].

Protein Extraction

Tissue extracts of human prostate epithelial cells maintained in tissue culture for one passage, and c-MYC infected huPrE cells were prepared by homogenization in 400 μl cold buffer A (10 mM HEPES pH 7.9; 10 mM KCl: 0.1 mM EDTA; 0.1 mM EGTA; 0.1 mM DTT; 1× protease complete (Roche, Indianapolis, IN). The cells were allowed to swell on ice for 15 min, after which 25 μl of a 10% solution of Nonidet NP-40 (Sigma) was added and the tube vortexed vigorously for 10 sec. The homogenate was then centrifuged for 30 sec in a Microfuge. The supernatant was snap frozen and stored at −70°C.

Western Blotting Analysis

Tissue extracts from huPrE epithelial cells grown in culture and their c-MYC infected counterparts as well as extracts from the BPH1 prostatic epithelial cell line were run on denaturing mini gels containing an acrylamide gradient from 4%–20% (w/v) polyacrylamide (Invitrogen). Gels were run in MOPS/SDS running buffer (50 mM 3-[*N*-morpholino] propane sulfonic acid [MOPS], 50 mM Tris base, 0.1% SDS, 1.025 mM EDTA [pH 7.7] for 35 min at 200 mA. Samples were blotted onto PVDF membrane (Invitrogen) using transfer buffer (25 mM bicine, 25 mM Bis-Tris, 1.025 mM EDTA, 50 nM chorobutanol [pH 7.2] (Invitrogen) in the mini gel tank according to the manufacturers instructions. Thereafter, membranes were blocked for 2–3 hr at room temperature in BLOTTO (5% nonfat dried milk powder [Difco]) dissolved in Phosphate buffered saline (Sigma) containing 0.1% Tween-20 (PBST). Membranes were incubated overnight in Blotto with the any one of the antibodies (anti c-MYC 1:800, AR 1:1,000, c-Myb 1:600, GFP 1:2,000, E-Cad 1:1,000, PTEN 1:800). Bound antibodies were detected using appropriate secondary antibodies (1:4,000 peroxidase conjugated Donkey anti rabbit/Sheep anti mouse [Amersham Pharmacia Biotech, Piscataway, NJ] and 1:2,000 rabbit anti goat [Santa Cruz]) and the enhanced chemiluminescence visualization system (Amersham Pharmacia Biotech) according to the manufacturer's instructions.

Immunohistochemistry

Deparaffinized, slide mounted sections were rehydrated and then subjected to heat induced antigen retrieval using the commercial retrieval buffer (H-3300) from Vector Laboratories, Brlingham, CA. The sections were microwaved for 15 min at a power that ensured continuous but not excessive boiling. Slides were permitted to cool to room temperature prior to incubation with 3% hydrogen peroxide in methanol for 15 min to block endogenous peroxidase. After washing in PBS the slides were blocked in Clean Vision™ from ImmunoVision Technologies for 15 min. This blocking optimized the use of monoclonal antibodies on tissue recombinants in which an immunocompromised mouse host was the graft host. The antibodies towards GFP (Santa Cruz,), Ki67, PSA, and broad spectrum Keratin (DAKO) were all used at 1:200 (p63 used at 1:1,000) [diluted in 1:4 normal swine serum (broad spectrum Keratin, PSA, p63) or normal rabbit serum (GFP, Ki67, keratins 8, 14, 18) in PBS/5% BSA]. All antibodies were incubated on sections overnight at 4°C. Sections were then incubated with the appropriate biotinylated secondary antibodies for 1 hr. [Broad spectrum Keratin, p63 and PSA, swine anti rabbit (DAKO), and for GFP, keratin 8, 14, 18 and Ki67 rabbit anti mouse, (DAKO), both of which were diluted 1:500 in the appropriate normal serum (see above)]. After appropriate washing steps the sections were incubated in ABC-HRP complex (Vector) for 30 min and washed extensively. Bound antibodies were then visualized by incubation with 3,3′-diaminobenzidine tetrahydrochloride (liquid DAB, DAKO). Sections were counter-

stained with hematoxylin. Images were captured onto a computer using a Zeiss microscope equipped with an AxioCam camera (Zeiss) and software.

Identification in Histological Sections of Species Origin of Cells in a Tissue Graft

Staining with the Hoechst 33258 dye (Sigma) was performed, as previously described [46]. The Hoechst dye Sections were examined by fluorescence microscopy. Host mouse cells contain several small discrete intranuclear fluorescent bodies, which are absent in cells from either rat or human allowing us to confirm that the tumor is not derived from the host mouse.

RNA Isolation

Tissue was rapidly excised from the outer portions of the graft and placed in 10x v/v RNA LATER (Ambion, Austin, TX). The tissue was then refrigerated prior to use 1–5 days after removal from the host. The tissue was dissected in a Petri dish containing RNA LATER to remove any kidney tissue (none was actually visible in any of the tissues) or obviously necrotic tissue (this tissue was very soft and white, resembling cotton candy).

RNA was isolated using the Qiagen mini RNA Easy kit according to the manufacturers instructions (Qiagen, Valencia, CA). The RNA was DNAse treated again using Qiagen reagents as detailed in the RNA easy protocol. The RNA concentration was then determined spectrophotometrically and the RNA aliquoted and snap frozen at −70°C.

RNA Labeling and Hybridization

All RNA and cDNA manipulations and cDNA array hybridizations were undertaken by technical support staff within the Vanderbilt Microarray Shared Resource (http://array.mc.vanderbilt.edu) using the protocols outlined on their website http://array.mc.vanderbilt.edu/support/protocols.htm. The use of tissue culture cells permitted the use of the standard cDNA labeling without amplification of the RNA. The microarray used for our experiments was the human 11K comprised of the Research Genetics human clone set.

cDNA Array Analysis

Data was normalized by Lowess sub grid and Gene Pix Pro Software was used to analyze differentially expressed genes between the two analysis groups. The groups consisted of huPrE grown in culture and infected with the LZRS-myc virus.

RESULTS

Infection of Hupre With a Retrovirus Containing C-Myc/Egfp Elicits Phenotypic Changes In Vitro

The huPrE cells grown on tissue culture plastic have a characteristic cobblestone appearance (Fig. 2). The presence of high levels of cholera toxin severely suppressed fibroblastic growth resulting in an almost pure epithelial cell population, as determined by visual examination. The rate of emergence of epithelial cell sheets from individual tissue fragments was highly variable both with respect to 'flask to flask' variation-using tissue from a single patient and with respect to

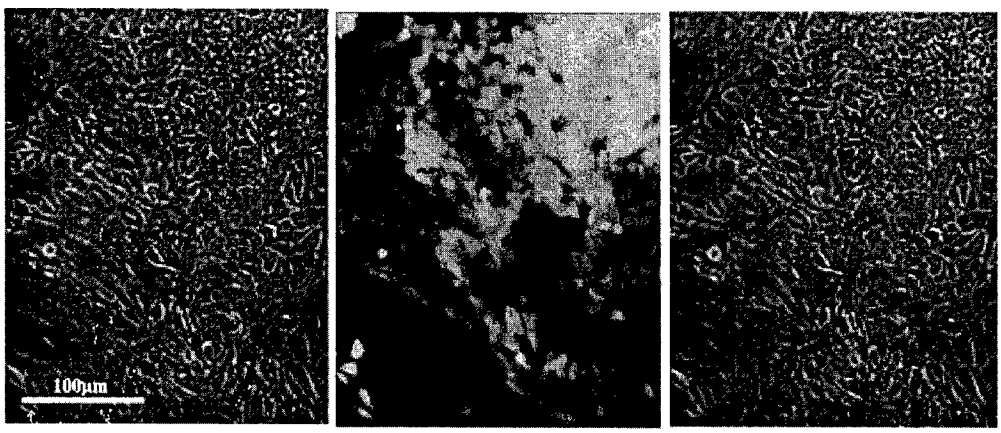

Fig. 2. Phase contrast photomicrograph of human prostate epithelium in cell culture 4 days after infection (Left panel). Note the typical cobblestone morphology in lower left hand side compared to the denser cells present in the upper right hand side. (Middle panel) Fluorescent image of human prostate epithelium culture 4 days post infection. Note that approximately one half of the cultured cells strongly express EGFP due to infection by the C7-Myc retrovirus. (Right panel) overlay, confirming that the small densely packed cells express EGFP while those with the cobblestone morphology do not.

'patient to patient' variation. Infection was started on day 2 in culture regardless of the presence/absence of visible epithelial cell outgrowths. After 2–5 rounds of infection a very large number of cells (20%–40%) on the margins of the growing sheet of epithelial cells expressed EGFP, suggesting an extremely efficient infection. At this point, infection was halted and the cells allowed to proliferate for 72 hr. The cultured cells displayed an altered morphology. Instead of a uniform monolayer of epithelial cells with a cobblestone appearance, there were discreet nests of tightly packed cells. The nests had well defined borders and were surrounded by cells displaying the expected normal phenotype (Fig. 2). When visualized on an inverted fluorescent microscope the nests displayed uniform EGFP fluorescence while the surrounding cells did not express EGFP.

All of the c-MYC/EGFP infected cell cultures observed (three patients from which both TZ and PZ cores were put into independent culture dishes in duplicate, a total of 12 independent cultures) exhibited similar morphological changes. The cells were irregular in shape and markedly smaller, the cytoplasm to nuclear ratio was decreased, and the nucleus was in many cases irregular in shape with prominent nucleoli. The cells also formed multiple layers within the nests, and many non-adherent viable cells were observed. The 'nest' phenomenon was observed until the cultures were trypsinized and split. Subsequent cultures initially displayed both phenotypes of cells but the morphologically normal cells were rapidly lost as the EGFP-expressing epithelial cells rapidly colonized the tissue culture plates. Within 10 days the entire culture consisted of EGFP expressing cells that varied widely in their fluorescence (and by subsequent analysis c-MYC expression). Over time the EGFP expression became more uniform but a range of EGFP expression has always been observed throughout the cultures. This suggests that the cultures represent a variety of clones resulting from multiple initial infections.

HuPrE infected with the LZRS C7Δ (the 'empty vector') exhibited normal cobblestone morphology and typically infect with relatively low efficiency $\leq$1% at low passage number, the control infections are less efficient than infections with the C7-Myc retrovirus. The Green EGFP infected cells were indistinguishable from their uninfected neighbors under phase contrast and could only be identified by EGFP expression. The C7Δ-infected cells could be passaged a maximum of five times before they became senescent.

The C7 Myc infected cells were maintained through 16 passages and showed no signs of senescence during this period. They continued to express both EGFP and c-MYC as well as prostatic epithelial markers including AR and PSA.

Hupre/C-Myc-Egfp Plus RugmTissue Recombinants Form Rapidly Growing Adenocarcinomas Expressing Human Prostatic Markers

Tissue recombinants of huPrE and rUGM were prepared. Control grafts contained either uninfected or C7-Δ-infected epithelium. Recombinants using C7-myc contained different percentages of c-MYC-infected cells (from 10% to 50% dependent on the time post infection that the cells were grafted). All grafts were composed of 100,000 epithelial cells and 300,000 rUGM cells. Host mice carrying myc-expressing grafts were sacrificed after 28 days due to the large size of the graft, which exceeded the size of the normal kidney (Fig. 3). Recombinants composed of C7Δ PrE and rUGM grafted to the contralateral kidneys of experimental hosts were very small and poorly developed at 28 days post grafting. In separate experiments, using a 3-month time point fully differentiated prostatic structures expressing PSA and AR were seen. Control grafts maintained a benign histology throughout (Fig. 3). The phenotype and timing of developmental events in these control grafts is consistent with previously published results using human prostatic epithelial organoids [47].

Initial inspection of the large c-MYC expressing grafts, indicated several very large blood vessels located on the surface of the graft and areas of white necrotic tissue in areas devoid of obvious blood vessels (Fig. 3). The kidney tissue was readily apparent upon subsequent dissection and was essentially normal.

C7-Myc cells grafted subcutaneously into the flank of SCID mice developed large tumors after 6 weeks (data not shown) that were indistinguishable from C7-Myc recombined with rUGM. The slightly longer time frame probably reflects the slower recruitment of blood vessels to a subcutaneous graft site compared to the sub renal graft site.

Thin smears of surface cells from the tumors expressed EGFP when exposed to fluorescent light (data not shown). These cells were placed into tissue culture to confirm EGFP expression and their human origin.

Expression from the CMV promoter is maintained throughout the growth of the graft. We have previously observed promoter downregulation (unpublished data) in cells carrying genes under the CMV promoter introduced via retroviral integration possibly via methylation events consistent with those described in transgenic mice [48,49]. The EGFP levels within the cells placed into reculture maintained a range of EGFP expression consistent with cultures prior to grafting suggesting that such repression had not occurred in these tumors.

In all the huPrE/c-MYC tumors the grafts consisted of cells strongly staining with hematoxylin. The cells characteristically exhibited large irregular nuclei, pro-

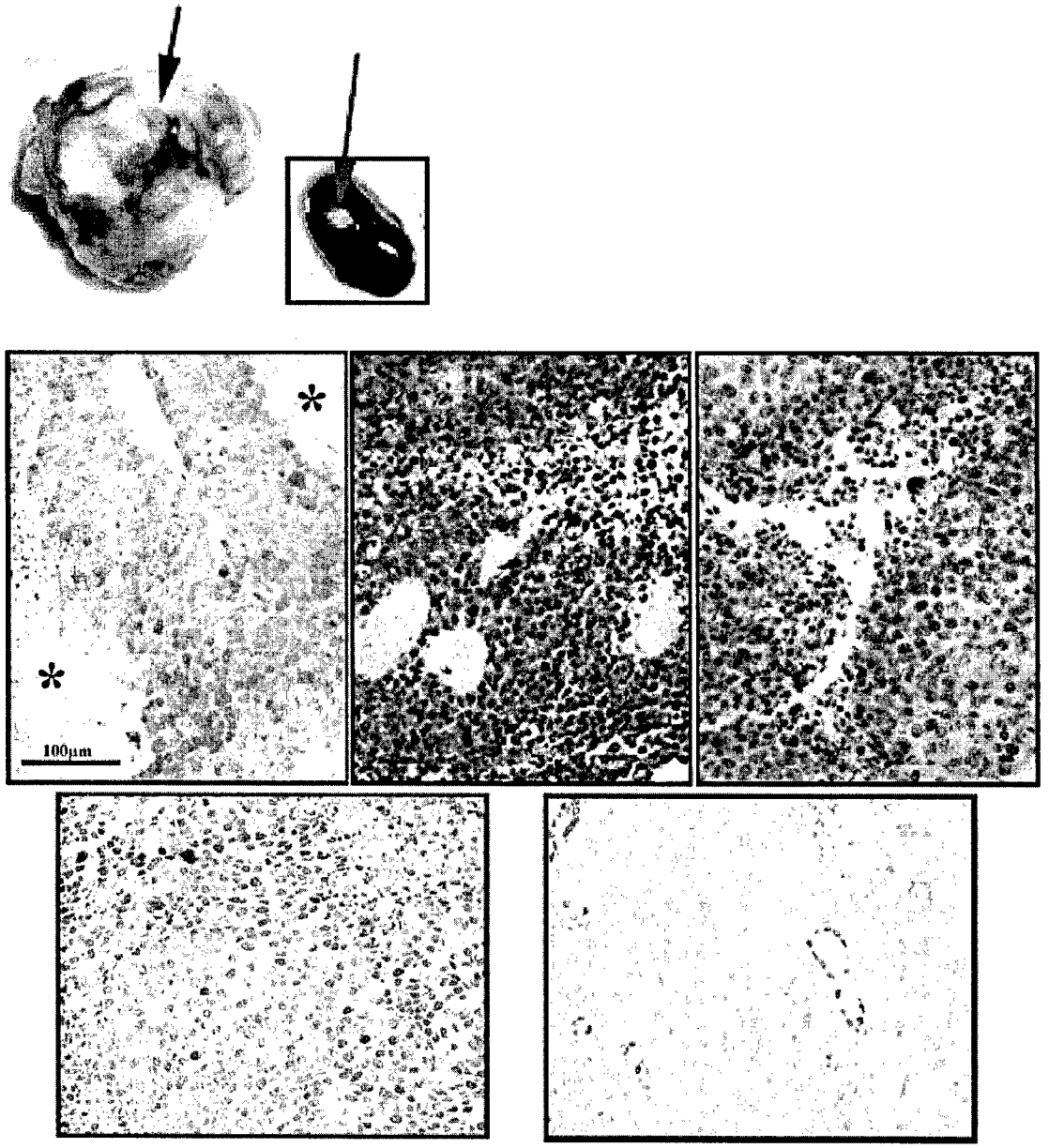

Fig. 3. Gross anatomy of mouse kidney with a c-MYC overexpressing prostate epithelial cell recombinant xenograft (top left). Note the encasement of the kidney by the tumor (black arrow). The control kidney carrying the C7Δ PrE/rUGM graft is displayed on the right, the small xenograft is barely visible (red arrow). Photomicrograph showing the poorly differentiated c-MYC expressing human prostatic tumors (middle/bottom panel) strongly express enhanced green fluorescent protein (middle left) PSA [(center)* indicates necrotic tissue]. The high mitotic rate observed in the tumor was confirmed by a very high index of statining with Ki67 (middle right). Bottom panel (left to right) AR, and p63.

minent nucleoli, and dense cytoplasm. A large number of dividing cells were present in a single field and many of the mitotic figures were clearly abnormal (Fig. 3). No fibromuscular stroma was present in the grafts nor was any apparent at the graft extremities. Irregular areas of necrotic tissues extended throughout the grafts and predominated in the interior, but did not interfere with the kidney. Areas of living tissue surrounded the few blood vessels that populated the graft interior. Immunohistochemical analysis of the C7-myc induced tumors revealed that these retained expression of two key markers of prostate tissue, AR and PSA. In addition the tumors expressed EGFP confirming their origin. Tumors expressed keratins 8 and 18 and lacked p63 and keratin 14 staining suggesting a luminal rather than basal cell origin. This is consistent with the profile seen

in human prostate cancer. The proliferation rate of the cells was extremely high as indicated by the almost universal presence of Ki67 in the nuclei (Fig. 3). This was consistent with the observation of extremely rapid tumor growth.

No infiltration was observed into the kidney, a well dealinated border was observed and the kidney morphology was normal with no obvious compression or damage (Fig. 3). Hoechst 33258 staining confirmed that none of the epithelial cells observed were of mouse origin and that no 'non mouse' cells were present in the kidney (data not shown). Some areas displaying p63 positive cells were observed within the graft, these were determined (by a trained pathologist) to be mouse kidney structures caught in cross section, providing a good internal positive control for the tumor cells, which were universally negative for basal cell markers (Fig. 3).

Molecular Characteristics of Tumor-Derived Cells

A microarray analysis comparison of the cells derived from the C7-myc tumors and of primary epithelial cultures from the same patient revealed a number of changes (Table 1). As might be expected many genes were seen to be regulated in response to c-MYC overexpression. Attention in this analysis was focused upon genes known to be regulated in tumors. Of particular note was the observation that PTEN and E-cadherin expression was seen to be suppressed and c-Myb expression was observed to be upregulated in the tumorigenic cells. This observation was confirmed by Western blotting to examine expression of these proteins (Fig. 5). Western blotting analysis also confirmed the continued overexpression of c-MYC, and the expression of both AR and EGFP.

DISCUSSION

The present study demonstrates that c-MYC overexpression is sufficient to drive normal human prostatic epithelium to a metastatic tumor within a tissue recombination model. Retroviral infection of normal prostate epithelium with the EGFP expressing empty vector resulted in benign prostatic architecture indicating that MYC overexpression not infection/integration

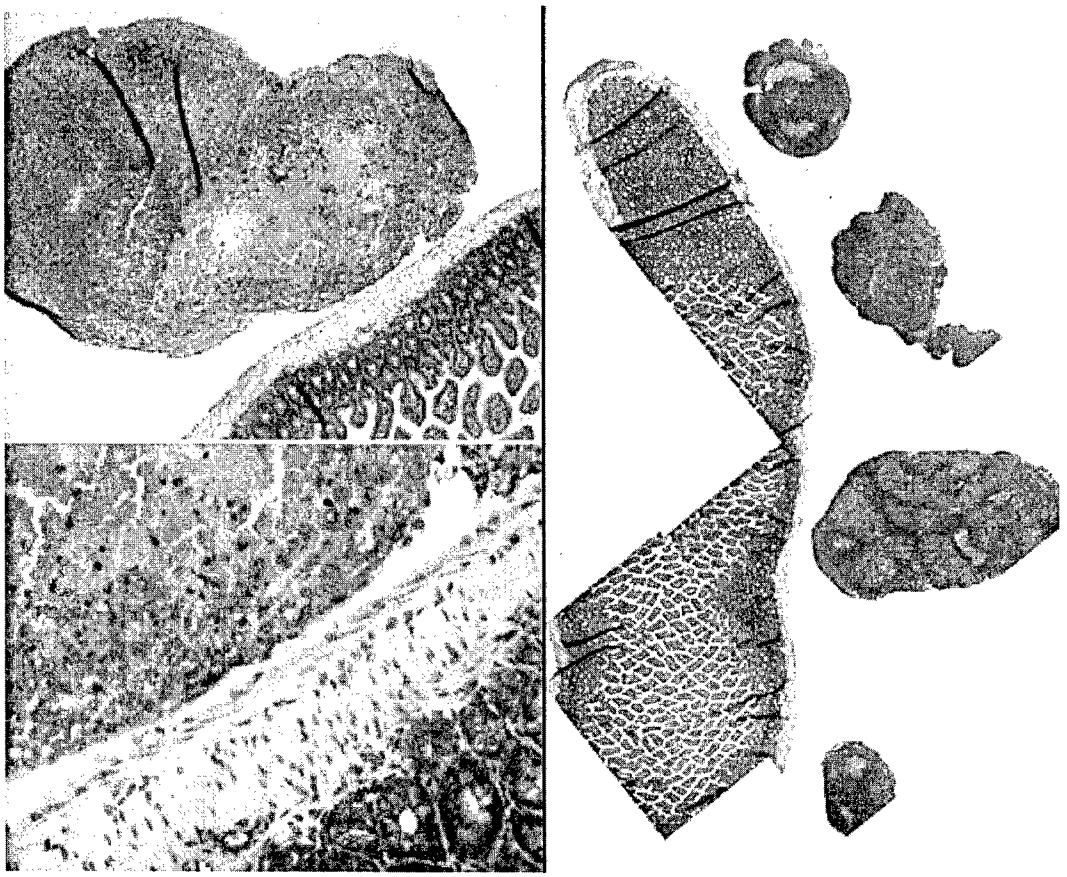

Fig. 4. Histopathologic appearance of metastatic lesions. Multiple metastatic lesions were found in mice as focal growths predominantly following the line of the intestinal tract. H&E high magnification of tumor immediately adjacent to the intestine (left panel top & bottom). Low magnification composite (right panel) showing three metastatic nodules that were attached to the host mouse intestine.

TABLE I. Microarray Data Set of mRNA Showing 2-fold Differences in Levels Between C7-Myc PrE and C7Δ PrE

Category	Gene	GenBank ID	Description	ACF
Transcription Factors	ARHE	NM_00518	Ras homolog gene	3.67
	MAFG	NM_00239	v-maf oncogene homolog G	3.27
	SON	NM_05818	Similarities with MYC MOS	−2.29
	HRASLS3	NM_00706	HRAS-like suppressor 3	−2.29
	TCF7	NM_00320	Transcription factor 7	
	TCF12	NM_00320	Transcription factor 12	−4.67
	VAV3	NM_00611	vav 3 oncogene	−1.36
	NFE2L2	NM_00616	Transcription factor	−2.53
	FOSL2	NM_00525	Dimerizes with JUN forming the transcription of factor complex AP-1	−1.65
	Notch3	NM_00871	Transcription factor	−3.64
	RABA1	NM_00416	Member RAS oncogene family	−1.78
Growth factors	INSL4	NM_00219	Member of the insulin superfamily	
	VEGF	NM_00337	Vascular endothelial growth factor	
Kinases	MKNK2	NM_01757	MAP kinase interacting serine/threonine kinase 2	−2.32
	SCAP1	NM_00372	Belongs to the src family kinases	−4.69
Adaptor molecules	NCK1	NM_00615	Adaptor protein involved in transducing signals from receptor tyrosine kinases to downstream recipients such as RAS	−1.67
	SP110	NM_08042	May have a role in the regulation of gene transcription	−2.28
	ABR	NM_02196	These proteins might interact with members of the Rho family	−2.68
	RNF4	NM_00293	RING finger protein, enhances AR-dependent transcription	−3.49
Apoptosis	BCL2A1	NM_00404	BCL2-related protein A1	−1.56
	PDCD4	NM_14534	Thought to play a role in apoptosis	−1.53
	CASP3	NM_00434	Caspase 3 apoptosis-related protease	
Extracellular matrix	ADAM15	NM_00381	A disintegrin and metalloproteinase domain 15 (metargidin)	−1.34
	TIMP1	NM_00325	Tissue inhibitor of MMP1	2.26
	MMP14	NM_00499	Matrix metalloproteinase activates MMP2 protein may be involved in tumor invasion	−1.71
	TIMP2		Tissue inhibitor of MMP 2	−2.71
Cell cycle	S100A10	NM_00296	Calcium-binding, involved in the regulation of cell cycle progression and differentiation	−2.23
	CDK4	NM_00007	Cyclin-dependent kinase 4	−1.75
Proliferation/ Differentiation	DUSP6	NM_00194	Gene product inactivates ERK2,	−1.95
	MAPRE2	NM_01426	Homology with APC suggests involvement in tumorigenesis and proliferative control of normal cells	−1.39
	SHC1	NM_18300	Couples activated growth factor receptors to a signaling pathway	−1.5
Proteases	Kallikrein 10	NM_00277	Serine proteases having diverse physiological functions	−1.72
	KLK5	NM_01242	Kallikrein 5	−1.59
	SPUVE	NM_00717	Protease, serine, 23	
	SLP1	NM_00306	Secreted serine protease inhibitor protects epithelial tissues	−5.04
	CSTA	NM_00521	Encodes a stefin that functions as a cysteine protease inhibotor	−4.65
Cytoskeleton/Motility	DSTN	NM_00687	Actin depolymerizing factor	−1.7
	CLDN1	NM_12110	Integral membrane protein component of tight junctions	−2.45
	CLDN4	NM_00130	Integral membrane protein, which belongs to the Claudine family	−1.33

(*Continued*)

TABLE I. (*Continued*)

Category	Gene	GenBank ID	Description	ACF
	THYB4	NM_02110	Actin sequestering protein, regulates actin polymerization, proliferation migration, and differentiation	−5.1
	LAMC2	NM_00556	Extracellular marrix glycrprotein, implicated in adhesion megration, differentiation, and metastasis	−1.5
	WIRE	NM_13326	Has a role in the WASP-mediated organization of the actin	−4.15
	KRT13	NM_15349	Keratin 13	−4.51
Neuronal	NDN	NM_00248	Mouse studies suggest a role in growth suppression in postmitotic neurons	−1.84
	SST Somatostatin	NM_00104	A regulator of endocrine and nervous system function	−1.97
Metastasis	p8	NM_01238	p8 protein (candidate of metastasis)	−1.94

of the EGFP expressing retrovirus induces the cancer phenotype. The tumors formed in this model retain some key characteristics of human prostate cancer, notably the expression of AR and PSA, and the ability to metastasize.

The c-MYC overexpression combined with a large percentage of infected cells produces a cancer phenotype within our xenograft model that is aggressive and progressive. The cells were obtained from tissue derived from aging males and may already have accumulated genetic hits that, of themselves, are insufficient to alter histology. The levels of c-MYC expressed by a CMV-driven retroviral delivery system would certainly constitute a very large additional molecular hit. The resulting tumors resemble a poorly differentiated advanced carcinoma, however, the growth rate is accelerated in comparison with the human disease. Myc expression can be a pivot point in the cellular decision-making process that determines if a cell will undergo proliferation or apoptosis [50–55]. Myc overexpression within the primary huPrE appears to be exhibiting a proliferative effect demonstrated by the extremely large number of Ki67 positive cells present within the renal capsule graft and the metastatic lesions. The lack of expression of the basal cell markers keratin 14 and p63 indicate that the c-Myc tumor, like human prostate adenocarcinoma, loses basal cells during tumor formation.

Similar c-MYC-based retroviral rodent models created by Thompson and co-workers [25–27,56–59] in prostate and by Edwards [60] in the breast lacked the aggressiveness of our model unless activated ras was also present. Less than 0.1% of epithelial cells carried the retrovirally introduced genes in the mouse TR's while our grafts contained 10%–50% infected cells thus altering the environment considerably as normal cells

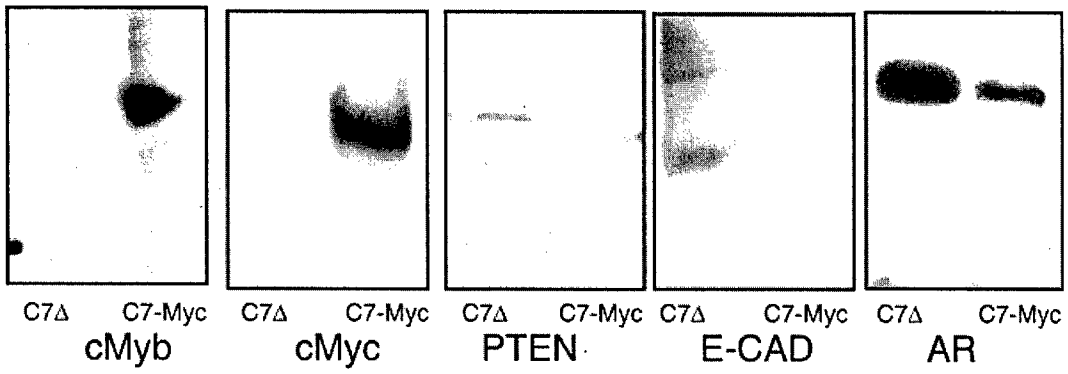

Fig. 5. Western blot analysis of C7-Myc and C7Δ infected cells. Western blot of human prostatic epithelial cells infected with C7-Myc or C7Δ (empty vector). All lanes contain 100 of protein except PTEN (250 μg). EGFP (Top left) is detected only in C7-Myc infected cells, C7Δ infected cells made up approximately 1% of the culture and while fluorescent cells were visible no signal was detected by western analysis. E-cadherin 120 kDa (top middle), Androgen receptor 130 kDa (Top right), cMyb 75 kDa (bottom left) c-MYC 67 kDa (bottom middle) PTEN 60 kDa (bottom right).

have the potential to inhibit the growth of transformed cells [61]. Microarray data do not indicate increased levels of ras mRNA within our C7-Myc tumors. Mouse strain backgrounds modify the effects of the oncogenes myc and ras [27] within the retrovirally infected TR's. By virtue of using human tissue, the present study examines an outbred epithelial cell population.

More recent transgenic mouse studies have demonstrated that the degree of response to c-MYC overexpression in mouse prostatic epithelium is dose related, with increased expression giving rise to more severe phenotypes [20,22]. All three described prostate-specific c-MYC-overexpressing mice develop mPIN. Mice expressing c-MYC using the Probasin promoter progress to invasive cancer in a time frame that is determined by the relative strength of the promoter construct used (ARR_2PB or sPB) [20]. Low levels of c-MYC expression are thought to cause prostatic dysplasia in the prostates of rats treated in the neonatal period with DES [62]. Progression beyond PIN is not observed within the lifetime of the C(3)Myc mouse. As serial recombination experiments using the C(3)-Myc mouse or the DES treated prostates have not been performed it is not known if these PIN-like lesions would progress over time as is thought to happen in humans. Our model possibly shows such an accelerated progression because the epithelium is already primed by both age related genetic changes and environmental/physiological events within the diseased prostate combined with expression of c-MYC from an extremely strong constitutive promoter.

Human prostatic epithelium expresses prostate specific antigen (PSA), in vivo this weak protease belongs to the large family of Kallikreins, and is not, despite the name, totally specific for the prostate. However, PSA is the main basis of the blood tests used to detect and monitor prostate cancer. PSA is androgen-regulated in normal and low-grade prostate cancers, however, as cancers progress to an androgen-independent state, PSA levels climb marking disease progression. Primary cultures of benign prostate cells initially express PSA as do the established cell line LNCaP [63]. However, it is commonly observed that cells in culture rapidly lose expression of steroid receptors, including AR, and consequently lose expression of steroid regulated gene products such as PSA. Tissue recombinants composed of normal prostatic epithelium and rUGM express both AR and PSA [47], as would be expected, since these genes are both regulated by the context in which the cell is growing. More remarkably Myc overexpressing cells express PSA and maintain their androgen receptor expression in culture. Tumors derived from these cells continue to express PSA and AR in vivo adding an important element to the relevance of this model.

Sawyers and co-workers [20] have identified a molecular signature that identifies both the c-MYC overexpressing prostate tumors present in their transgenic mouse model and a subset of human prostate tumors that overexpress Myc. Our cDNA analysis identified several targets that were subsequently analyzed by Western blotting, as our cDNA array differed from that used by the Sawyers group we were unable to compare their molecular signature with the one we obtained. We were however able to use the microarray data to identify proteins previously shown to be involved in tumorigenesis which were regulated in this model. Western blot analysis was used to confirm microarray data on the loss of PTEN and E-cadherin in the c-MYC expressing cells. Both of these proteins are implicated as playing a tumor suppressive role in cancer development and show a marked decrease in expression compared to control cells. Decreased or absent E-cadherin expression is a frequent occurrence in human prostate cancer [64] and this is recapitulated within our myc overexpressing tumor. The undetectable levels (by Western blotting) of E-cadherin present in our myc tumor cells in culture may represent a general loss of adhesion, which would in part explain the low adhesion of the cells both to the tissue culture plastic and other cells resulting in loss of the cobblestone morphology and lack of strong junctions between cells. Immunohistochemistry on the tumor tissue failed to pick up E-cadherin staining on the cell membranes within the tumor (data not shown).

PTEN is a tumor suppressor gene situated at 10q23, a deletion hot spot in prostate cancer [65]. PTEN Knockout mice are embryonic lethal [66] but tissue specific homozygotes (0% gene dose in prostate 100% in most other tissues) and the newer hypomorphic mice (25%–35% gene dose) [67–70] display mPIN that progresses to invasive carcinoma over time. Heterozygote PTEN deletion results in mPIN but requires the presence of a second genetic lesion to progress to an invasive cancer phenotype [71,72]. PTEN encodes a lipid phosphatase that inhibits the PI3 kinase/AKT pathway. The AKT pathway is a pivotal point in the control of cellular homeostasis. Many pathways including TGFβ, IGF, EGF and Ras interact with AKT. The activation of AKT appears to indirectly promote androgen-independent survival of prostate cancer cells, but the mechanism is as yet undetermined [73,74]. PTEN and AKT are upstream of c-MYC; PTEN loss causes upregulation of AKT that in turn upregulates c-MYC. The role of AKT on AR and subsequent repercussions on c-MYC are unknown but the importance of AKT and by extension PTEN in androgen independent growth of prostate cancer correlates with the role of c-MYC.

Microarray data verified by Western blot analysis demonstrated upregulation of the cMyb oncogene in

the C7-Myc model. Myb is usually regarded as a proto-oncogene within the hematopoietic line where it functions as a cell cycle promoter. c-Myb inhibits expression of $p15^{ink4b}$ while transactivating c-MYC, Bcl-2, COX2, IGF-I, and IGF-IR [75–77]. While c-Myb has primarily been studied in the hematopoietic lineage it is also expressed in breast, the gastrointestinal lineage [78], and prostate [79–81], it is upregulated in cancers and some premalignant lesions of these tissues [79,80,82–85]. The upregulation of cMyb in the C7-Myc model may further enhance the transforming ability of c-MYC by stimulating pathways that are not stimulated by Myc.

This work demonstrates the application of retroviral infection strategy followed by tissue recombination to examine the contribution of individual gene products to carcinogenesis. The approach can be used on any of the regulated products within the 8q24 amplicon, or those identified in the cDNA microarray analysis, both alone and in combination to determine their contribution to the final graft phenotype. This in vivo model of prostate cancer based upon human prostatic epithelium has many interesting and potentially useful features. However, the rapid progression and extremely high proliferative rate limits the ability to examine early tumorigenic events. The model retains many characteristics of human prostate cancer including continued expression of AR and PSA. The model also demonstrates downregulation of two tumor suppressors (PTEN and E-cadherin), which are suppressed in human prostate cancer and shows upregulation of Myb, which is known to be upregulated in the human disease. Metastasis is also an important component of the in vivo model. Cell cultures derived from both the initial viral infections and from the tumors retain many of these important characteristics and represent a potentially useful resource to examine prostate cancer biology. We are working to modify the model using a series of weaker constitutive, conditional, and regulatible promoters that will better allow us to follow stages of progression.

ACKNOWLEDGMENTS

Preliminary feasibility studies were supported by a grant to S.W.H and Y.F.L from the University of California, San Francisco Prostate Cancer Center. This work was supported by a postdoctoral fellowship grant DAMD 17-01-1-0037 to KW from the Department of Defense Prostate Cancer Research Program by NIH grant CA96403 and support from the Joe C. Davis Foundation to S.W.H. All microarray experiments were performed in the Vanderbilt Microarray Shared Resource. All DNA sequencing took place in the Vanderbilt DNA Sequencing Facility. Both core resources are supported in part by the Vanderbilt Ingram Cancer Center (P30 CA68485) and the Vanderbilt Diabetes Research and Training Center (P60 DK20593). SWH and KW wish to express their personal gratitude to Dr. Peter Carroll of UCSF for his unhesitating and selfless support.

REFERENCES

1. Quinn M, Babb P. Patterns and trends in prostate cancer incidence, survival, prevalence and mortality. Part I: International comparisons. BJU Int 2002;90(2):162–173.
2. Hsing AW, Tsao L, Devesa SS. International trends and patterns of prostate cancer incidence and mortality. Int J Cancer 2000; 85(1):60–67.
3. Chiarodo A. National Cancer Institute roundtable on prostate cancer: Future research directions. Cancer Res 1991;51(9):2498–2505.
4. Carroll PR. Trends in prostate cancer mortality among black men and white men in the United States. In: Chu KC, Tarone RE, Freeman HP, editors. Center to reduce cancer health disparities. Bethesda, MD: National Cancer Institute, Cancer 2003;97:1507–1516 (Urol Oncol 2003;21(6):483–484).
5. Lau YF, Lau HW, Komuves LG. Expression pattern of a gonadoblastoma candidate gene suggests a role of the Y chromosome in prostate cancer. Cytogenet Genome Res 2003;101(3–4):250–260.
6. DeMarzo AM, Nelson WG, Isaacs WB, Epstein JI. Pathological and molecular aspects of prostate cancer. Lancet 2003;361(9361): 955–964.
7. Malynn BA, de Alboran IM, O'Hagan RC, Bronson R, Davidson L, DePinho RA, Alt FW. N-myc can functionally replace c-myc in murine development, cellular growth, and differentiation. Genes Dev 2000;14(11):1390–1399.
8. Davis AC, Wims M, Spotts GD, Hann SR, Bradley A. A null c-myc mutation causes lethality before 10.5 days of gestation in homozygotes and reduced fertility in heterozygous female mice. Genes Dev 1993;7(4):671–682.
9. Davis A, Bradley A. Mutation of N-myc in mice: What does the phenotype tell us? Bioessays 1993;15(4):273–275.
10. Blackwood EM, Eisenman RN. Max: A helix-loop-helix zipper protein that forms a sequence-specific DNA-binding complex with Myc. Science 1991;251(4998):1211–1217.
11. Hurlin PJ, Queva C, Koskinen PJ, Steingrimsson E, Ayer DE, Copeland NG, Jenkins NA, Eisenman RN. Mad3 and Mad4: Novel Max-interacting transcriptional repressors that suppress c-myc dependent transformation and are expressed during neural and epidermal differentiation. Embo J 1995;14(22):5646–5659.
12. Bowen H, Biggs TE, Phillips E, Baker ST, Perry VH, Mann DA, Barton CH. c-Myc represses and Miz-1 activates the murine natural resistance-associated protein 1 promoter. J Biol Chem 2002;277(38):34997–35006.
13. Gartel AL, Shchors K. Mechanisms of c-myc-mediated transcriptional repression of growth arrest genes. Exp Cell Res 2003; 283(1):17–21.
14. Peukert K, Staller P, Schneider A, Carmichael G, Hanel F, Eilers M. An alternative pathway for gene regulation by Myc. Embo J 1997;16(18):5672–5686.
15. Beier R, Burgin A, Kiermaier A, Fero M, Karsunky H, Saffrich R, Moroy T, Ansorge W, Roberts J, Eilers M. Induction of cyclin E-cdk2 kinase activity, E2F-dependent transcription and cell

growth by Myc are genetically separable events. Embo J 2000; 19(21):5813–5823.

16. Coller HA, Grandori C, Tamayo P, Colbert T, Lander ES, Eisenman RN, Golub TR. Expression analysis with oligonucleotide microarrays reveals that MYC regulates genes involved in growth, cell cycle, signaling, and adhesion. Proc Natl Acad Sci USA 2000;97(7):3260–3265.
17. Bouchard C, Thieke K, Maier A, Saffrich R, Hanley-Hyde J, Ansorge W, Reed S, Sicinski P, Bartek J, Eilers M. Direct induction of cyclin D2 by Myc contributes to cell cycle progression and sequestration of p27. Embo J 1999;18(19):5321–5333.
18. Herold S, Wanzel M, Beuger V, Frohme C, Beul D, Hillukkala T, Syvaoja J, Saluz HP, Haenel F, Eilers M. Negative regulation of the mammalian UV response by Myc through association with Miz-1. Mol Cell 2002;10(3):509–521.
19. Staller P, Peukert K, Kiermaier A, Seoane J, Lukas J, Karsunky H, Moroy T, Bartek J, Massague J, Hanel F, Eilers M. Repression of p15INK4b expression by Myc through association with Miz-1. Nat Cell Biol 2001;3(4):392–399.
20. Ellwood-Yen K, Graeber TG, Wongvipat J, Iruela-Arispe ML, Zhang J, Matusik R, Thomas GV, Sawyers CL. Myc-driven murine prostate cancer shares molecular features with human prostate tumors. Cancer Cell 2003;4(3):223–238.
21. Nesbit CE, Tersak JM, Prochownik EV. MYC oncogenes and human neoplastic disease. Oncogene 1999;18(19):3004–3016.
22. Zhang X, Lee C, Ng PY, Rubin M, Shabsigh A, Buttyan R. Prostatic neoplasia in transgenic mice with prostate-directed overexpression of the c-myc oncoprotein. Prostate 2000;43(4): 278–285.
23. Pelengaris S, Littlewood T, Khan M, Elia G, Evan G. Reversible activation of c-Myc in skin: Induction of a complex neoplastic phenotype by a single oncogenic lesion. Mol Cell 1999;3(5): 565–577.
24. Jensen NA, Pedersen KM, Lihme F, Rask L, Nielsen JV, Rasmussen TE. Mitchelmore C. Astroglial c-Myc overexpression predisposes mice to primary malignant gliomas. J Biol Chem 2003;278(10):8300–8308.
25. Thompson TC, Park SH, Timme TL, Ren C, Eastham JA, Donehower LA, Bradley A, Kadmon D, Yang G. Loss of p53 function leads to metastasis in ras+myc-initiated mouse prostate cancer. Oncogene 1995;10(5):869–879.
26. Thompson TC, Southgate J, Kitchener G, Land H. Multistage carcinogenesis induced by ras and myc oncogenes in a reconstituted organ. Cell 1989;56(6):917–930.
27. Thompson TC, Timme TL, Kadmon D, Park SH, Egawa S, Yoshida K. Genetic predisposition and mesenchymal–epithelial interactions in ras+myc-induced carcinogenesis in reconstituted mouse prostate. Mol Carcinog 1993;7(3):165–179.
28. Fleming WH, Hamel A, MacDonald R, Ramsey E, Pettigrew NM, Johnston B, Dodd JG, Matusik RJ. Expression of the c-myc protooncogene in human prostatic carcinoma and benign prostatic hyperplasia. Cancer Res 1986;46(3):1535–1538.
29. Jain M, Arvanitis C, Chu K, Dewey W, Leonhardt E, Trinh M, Sundberg CD, Bishop JM, Felsher DW. Sustained loss of a neoplastic phenotype by brief inactivation of MYC. Science 2002; 297(5578):102–104.
30. Karlsson A, Giuriato S, Tang F, Fung-Weier J, Levan G, Felsher DW. Genomically complex lymphomas undergo sustained tumor regression upon MYC inactivation unless they acquire novel chromosomal translocations. Blood 2003;101(7): 2797–2803.
31. Elo JP, Visakorpi T. Molecular genetics of prostate cancer. Ann Med 2001;33(2):130–141.
32. Tsuchiya N, Kondo Y, Takahashi A, Pawar H, Qian J, Sato K, Lieber MM, Jenkins RB. Mapping and gene expression profile of the minimally overrepresented 8q24 region in prostate cancer. Am J Pathol 2002;160(5):1799–1806.
33. Porkka KP, Tammela TL, Vessella RL, Visakorpi T. RAD21 and KIAA0196 at 8q24 are amplified and overexpressed in prostate cancer. Genes Chromosomes Cancer 2004;39(1): 1–10.
34. Reiter RE, Sato I, Thomas G, Qian J, Gu Z, Watabe T, Loda M, Jenkins RB. Coamplification of prostate stem cell antigen (PSCA) and MYC in locally advanced prostate cancer. Genes Chromosomes Cancer 2000;27(1):95–103.
35. El Gedaily A, Bubendorf L, Willi N, Fu W, Richter J, Moch H, Mihatsch MJ, Sauter G, Gasser TC. Discovery of new DNA amplification loci in prostate cancer by comparative genomic hybridization. Prostate 2001;46(3):184–190.
36. Bubendorf L, Kononen J, Koivisto P, Schraml P, Moch H, Gasser TC, Willi N, Mihatsch MJ, Sauter G, Kallioniemi OP. Survey of gene amplifications during prostate cancer progression by high-throughout fluorescence in situ hybridization on tissue microarrays. Cancer Res 1999;59(4):803–806.
37. Qian J, Jenkins RB, Bostwick DG. Detection of chromosomal anomalies and c-myc gene amplification in the cribriform pattern of prostatic intraepithelial neoplasia and carcinoma by fluorescence in situ hybridization. Mod Pathol 1997;10(11):1113–1119.
38. Chaib H, Cockrell EK, Rubin MA, Macoska JA. Profiling and verification of gene expression patterns in normal and malignant human prostate tissues by cDNA microarray analysis. Neoplasia 2001;3(1):43–52.
39. Buttyan R, Sawczuk IS, Benson MC, Siegal JD, Olsson CA. Enhanced expression of the c-myc protooncogene in high-grade human prostate cancers. Prostate 1987;11(4):327–337.
40. Hayward SW, Haughney PC, Lopes ES, Danielpour D, Cunha GR. The rat prostatic epithelial cell line NRP-152 can differentiate in vivo in response to its stromal environment. Prostate 1999; 39(3):205–212.
41. Wang YZ, Sudilovsky D, Zhang B, Haughney PC, Rosen MA, Wu DS, Cunha TJ, Dahiya R, Cunha GR, Hayward SW. A human prostatic epithelial model of hormonal carcinogenesis. Cancer Res 2001;61:6064–6072.
42. Hallowes RC, Bone EJ, Jones W. A new dimension in the culture of human breast. In: Richards RJ, Rajan KT, editors. Tissue culture in medical research. Vol 2. Oxford: Pergamon Press; 1980. pp 213–220.
43. Hayward SW. A simple method for freezing and storing viable tissue fragments. In Vitro Cell Dev Biol Anim 1998;34(1): 28–29.
44. Taylor-Papadimitriou J, Stampfer M, Bartek J, Lewis A, Boshell M, Lane EB, Leigh IM. Keratin expression in human mammary epithelial cells cultured from normal and malignant tissue: Relation to in vivo phenotypes and influence of medium. J Cell Sci 1989;94:403–413.
45. Perkins W, Campbell I, Leigh IM, MacKie RM. Keratin expression in normal skin and epidermal neoplasms demonstrated by a panel of monoclonal antibodies. J Cutan Pathol 1992; 19(6):476–482.
46. Cunha GR, Vanderslice KD. Identification in histological sections of species origin of cells from mouse, rat and human. Stain Technol 1984;59(1):7–12.

47. Hayward SW, Haughney PC, Rosen MA, Greulich KM, Weier HU, Dahiya R, Cunha GR. Interactions between adult human prostatic epithelium and rat urogenital sinus mesenchyme in a tissue recombination model. Differentiation 1998;63(3):131–140.
48. Snibson KJ, Woodcock D, Orian JM, Brandon MR, Adams TE. Methylation and expression of a metallothionein promoter ovine growth hormone fusion gene (MToGH1) in transgenic mice. Transgenic Res 1995;4(2):114–122.
49. Smith MR, Biggar S, Hussain M. Prostate-specific antigen messenger RNA is expressed in non-prostate cells: Implications for detection of micrometastases. Cancer Res 1995;55(12):2640–2644.
50. Pelengaris S, Khan M, Evan GI. Suppression of Myc-induced apoptosis in beta cells exposes multiple oncogenic properties of Myc and triggers carcinogenic progression. Cell 2002;109(3): 321–334.
51. Prendergast GC. Mechanisms of apoptosis by c-Myc. Oncogene 1999;18(19):2967–2987.
52. Prendergast GC. Myc and Myb: Are the veils beginning to lift? Oncogene 1999;18(19):2914–2915.
53. Dang CV, Resar LM, Emison E, Kim S, Li Q, Prescott JE, Wonsey D, Zeller K. Function of the c-Myc oncogenic transcription factor. Exp Cell Res 1999;253(1):63–77.
54. Dang CV. c-Myc target genes involved in cell growth, apoptosis, and metabolism. Mol Cell Biol 1999;19(1):1–11.
55. Amati B, Alevizopoulos K, Vlach J. Myc and the cell cycle. Front Biosci 1998;3:D250–D268.
56. Thompson TC. Growth factors and oncogenes in prostate cancer. Cancer Cells 1990;2(11):345–354.
57. Thompson TC, Egawa S, Kadmon D, Miller GJ, Timme TL, Scardino PT, Park SH. Androgen sensitivity and gene expression in ras + myc-induced mouse prostate carcinomas. J Steroid Biochem Mol Biol 1992;43(1–3):79–85.
58. Thompson TC, Kadmon D, Timme TL, Merz VW, Egawa S, Krebs T, Scardino PT, Park SH. Experimental oncogene induced prostate cancer. Cancer Surv 1991;11:55–71.
59. Lehr JE, Pienta KJ, Yamazaki K, Pilat MJ. A model to study c-myc and v-H-ras induced prostate cancer progression in the Copenhagen rat. Cell Mol Biol (Noisy-le-grand) 1998;44(6): 949–959.
60. Edwards PA, Ward JL, Bradbury JM. Alteration of morphogenesis by the v-myc oncogene in transplants of mammary gland. Oncogene 1988;2(4):407–412.
61. Mehta PP, Bertram JS, Loewenstein WR. Growth inhibition of transformed cells correlates with their junctional communication with normal cells. Cell 1986;44(1):187–196.
62. Pylkkanen L, Makela S, Valve E, Harkonen P, Toikkanen S, Santti R. Prostatic dysplasia associated with increased expression of c-myc in neonatally estrogenized mice. J Urol 1993;149(6): 1593–1601.
63. Denmeade SR, Sokoll LJ, Dalrymple S, Rosen DM, Gady AM, Bruzek D, Ricklis RM, Isaacs JT. Dissociation between androgen responsiveness for malignant growth vs. expression of prostate specific differentiation markers PSA, hK2, and PSMA in human prostate cancer models. Prostate 2003;54(4):249–257.
64. Umbas R, Schalken JA, Aalders TW, Carter BS, Karthaus HF, Schaafsma HE, Debruyne FM, Isaacs WB. Expression of the cellular adhesion molecule E-cadherin is reduced or absent in high-grade prostate cancer. Cancer Res 1992;52(18):5104–5109.
65. Verma RS, Manikal M, Conte RA, Godec CJ. Chromosomal basis of adenocarcinoma of the prostate. Cancer Invest 1999;17(6): 441–447.
66. Di Cristofano A, Pesce B, Cordon-Cardo C, Pandolfi PP. Pten is essential for embryonic development and tumour suppression. Nat Genet 1998;19(4):348–355.
67. Backman SA, Ghazarian D, So K, Sanchez O, Wagner KU, Hennighausen L, Suzuki A, Tsao MS, Chapman WB, Stambolic V, Mak TW. Early onset of neoplasia in the prostate and skin of mice with tissue-specific deletion of Pten. Proc Natl Acad Sci USA 2004;101(6):1725–1730.
68. Dose of PTEN Gene Drives Progression of Prostate Cancer. PLoS Biol 2003;1(3):E70.
69. Trotman LC, Niki M, Dotan ZA, Koutcher JA, Cristofano AD, Xiao A, Khoo AS, Roy-Burman P, Greenberg NM, Dyke TV, Cordon-Cardo C, Pandolfi P. Pten Dose Dictates Cancer Progression in the Prostate. PLoS Biol 2003;1(3):E59.
70. Wang S, Gao J, Lei Q, Rozengurt N, Pritchard C, Jiao J, Thomas GV, Li G, Roy-Burman P, Nelson PS, Liu X, Wu H. Prostate-specific deletion of the murine Pten tumor suppressor gene leads to metastatic prostate cancer. Cancer Cell 2003;4(3): 209–221.
71. Di Cristofano A, De Acetis M, Koff A, Cordon-Cardo C, Pandolfi PP. Pten and p27KIP1 cooperate in prostate cancer tumor suppression in the mouse. Nat Genet 2001;27(2):222–224.
72. Abate-Shen C, Banach-Petrosky WA, Sun X, Economides KD, Desai N, Gregg JP, Borowsky AD, Cardiff RD, Shen MM. Nkx3.1; Pten mutant mice develop invasive prostate adenocarcinoma and lymph node metastases. Cancer Res 2003;63(14): 3886–3890.
73. Nan B, Snabboon T, Unni E, Yuan XJ, Whang YE, Marcelli M. The PTEN tumor suppressor is a negative modulator of androgen receptor transcriptional activity. J Mol Endocrinol 2003;31(1): 169–183.
74. Ghosh PM, Malik S, Bedolla R, Kreisberg JI. Akt in prostate cancer: Possible role in androgen-independence. Curr Drug Metab 2003;4(6):487–496.
75. Wolff L, Schmidt M, Koller R, Haviernik P, Watson R, Bies J, Maciag K. Three genes with different functions in transformation are regulated by c-Myb in myeloid cells. Blood Cells Mol Dis 2001;27(2):483–488.
76. Ramsay RG, Friend A, Vizantios Y, Freeman R, Sicurella C, Hammett F, Armes J, Venter D. Cyclooxygenase-2, a colorectal cancer nonsteroidal anti-inflammatory drug target, is regulated by c-MYB. Cancer Res 2000;60(7):1805–1809.
77. Baserga R, Hongo A, Rubini M, Prisco M, Valentinis B. The IGF-I receptor in cell growth, transformation and apoptosis. Biochim Biophys Acta 1997;1332(3):F105–F126.
78. Zorbas M, Sicurella C, Bertoncello I, Venter D, Ellis S, Mucenski ML, Ramsay RG. c-Myb is critical for murine colon development. Oncogene 1999;18(42):5821–5830.
79. Rijnders AW, van der Korput JA, van Steenbrugge GJ, Romijn JC, Trapman J. Expression of cellular oncogenes in human prostatic carcinoma cell lines. Biochem Biophys Res Commun 1985;132(2): 548–554.
80. Edwards J, Krishna NS, Witton CJ, Bartlett JM. Gene amplifications associated with the development of hormone-resistant prostate cancer. Clin Cancer Res 2003;9(14):5271–5281.
81. Katz AE, Benson MC, Wise GJ, Olsson CA, Bandyk MG, Sawczuk IS, Tomashefsky P, Buttyan R. Gene activity during the early phase of androgen-stimulated rat prostate regrowth. Cancer Res 1989;49(21):5889–5894.
82. Guerin M, Sheng ZM, Andrieu N, Riou G. Strong association between c-myb and oestrogen-receptor expression in human breast cancer. Oncogene 1990;5(1):131–135.

83. Guerin M, Barrois M, Riou G. [The expression of c-myb is strongly associated with the presence of estrogen and progesterone receptors in breast cancer]. C R Acad Sci III 1988;307(20): 855–861.

84. Ramsay RG, Thompson MA, Hayman JA, Reid G, Gonda TJ, Whitehead RH. Myb expression is higher in malignant human colonic carcinoma and premalignant adenomatous polyps than in normal mucosa. Cell Growth Differ 1992;3(10): 723–730.

85. Thompson MA, Flegg R, Westin EH, Ramsay RG. Microsatellite deletions in the c-myb transcriptional attenuator region associated with over-expression in colon tumour cell lines. Oncogene 1997;14(14):1715–1723.